

# TYPHOON DAMAGE MAPPING USING NORMALIZED DIFFERENCED SPATIAL AUTOCORRELATION AND PLANETSCOPE IMAGE

A. C. Blanco<sup>1,2</sup>

<sup>1</sup>Philippine Space Agency, UP Diliman, Quezon City, Philippines – ariel.blanco@philsa.gov.ph

<sup>2</sup>Department of Geodetic Engineering, University of the Philippines Diliman, Quezon City, Philippines – acblanco@up.edu.ph

Commission III, WG IVa

**KEY WORDS:** Damage assessment, LISA, Local Moran's I, change detection, building damage

## ABSTRACT:

Damages to built and natural environments are essentially changes that needs to be detected and quantified. This is particularly true for the change detection approach. While the use of vegetation indices is effective for such assessment in natural or vegetated areas, the use of built-up indices does not yield useful results. This is because there is usually no significant reduction in materials. However, typhoon-damaged buildings are usually characterized by a change in form, shape, color, and texture. In this study, we examined the use of local spatial autocorrelation (LSA) to evaluate the level of damage to buildings. In particular, the local Moran's I was used, and an index called the normalized difference spatial autocorrelation (NDSA) was developed. Similar with other indices, the values are within the range of -1 to 1. NDSA using local Getis-Ord  $G_i^*$  and local Geary's  $C$  were also generated. With the observation that LSA generally decreases due to damages (especially to manmade structures), positive NDSA identifies the damage areas. The magnitude of the values corresponded to the level or degree of damage sustained as interpreted from very high-resolution satellite image. It was noted that the manual tagging of damages had missed buildings which are clearly damaged or destroyed based on the visual comparison of pre- and post-typhoon satellite images. This illustrates the value of the NDSA not only to assess damage on its own but also for guiding manual tagging from image and prioritizing post-disaster needs assessment and recovery operation.

## 1. INTRODUCTION

Typhoons typically bring destruction, including damages to properties and loss of lives. Mapping and assessment of damages to built and natural environments is critical to further understanding the destructive nature of typhoons and effectively allocate efforts towards relief and recovery. Several studies on mapping damages due to typhoons and other natural calamities (e.g., earthquake) have been undertaken (see Planck, 2014, Antonietta et al., 2015, Boschetti et al., 2015, Hoque et al., 2017, Adriano et al., 2019, Xu et al., 2019, Jimenez-Jimenez et al., 2020, McCarthy et al., 2020, Tay et al., 2020, Liu et al., 2021). While Hoque (2017) noted that the use of synthetic aperture radar (SAR) in tropical cyclone disaster management research was limited, we note that with Sentinel-1 being freely available, the utilization of SAR images is increasing. This is largely due to the all-weather capability of SAR systems. However, as noted by Antonietta et al. (2015), optical images are preferred for high level-of-detail damage assessments and the only option when visual interpretation must be utilized for post-typhoon assessment. Visual interpretation for damage mapping is time-consuming but nonetheless relatively easy when very high-resolution (submeter) images are used. However, as pointed out by Xu et al. (2019), "manual digitization is labor-intensive, requiring trained image analysts, is unsuitable for large areas, and is prone to inconsistencies related to human errors due to fatigue or quality control". The task becomes much more difficult when applied to high-resolution (resolution of a few meters) images (e.g., PlanetScope, RapidEye). There is the need to develop a methodology for assessing damage using such images as they become pervasive and more available.

Recent works have investigated the use of machine learning and deep learning in building damage assessment. Typically, the objective is to map damage buildings using a single image acquired post-disaster. This is exemplified by the work of Xu et

al. (2019) where WorldView 2 and 3 images were utilized. PlanetScope imagery and artificial intelligence has been used for extracting building inventory information (Kaplan, Kaplan, 2021) and assessing building damage (Adriano et al., 2019). The latter work utilized PlanetScope images in a data fusion manner which can be limiting for user with no access to other datasets. In terms of damage assessment, particularly for buildings, there are only a few studies conducted on the use of PlanetScope images.

Change detection as an approach for damage assessment is still considered a viable way to provide needed information on the extent and severity of damages. However, care must be taken as images immediate available after an event "may have variations in illumination due to cloud cover, different viewing angle compared to pre-event images, and spatial co-registration variations leading to difficulties in identifying structural damages, changed or affected areas by directly comparing thematic maps" (Vijayaraj et al., 2008). To address these, various studies have utilized structural and textural features which are not significantly affected variations in conditions pre- and post-events, among others. These features include local binary pattern, local edge pattern, and Gabor texture features (see Vijayaraj et al., 2008) and object-level homogeneity index (see Liu & Li, 2019). Spatial autocorrelation, the correlation among values of a variable due to the relatively close locational positions on a two-dimensional surface (Griffith, 1987), has been used in change detection studies (see Zhou et al., 2016, Mondini, 2017).

In this study, the use of PlanetScope image for damage mapping was explored using local indicators of spatial autocorrelation. The central and southern parts of the Philippines was heavily hit by Typhoon Rai (local name: Odette), a category 5 typhoon. Image search indicated that there are available useable PlanetScope images a few days after the typhoon. This effort addresses the need for data and information on damages.

## 1.1 Study Area

Talisay City in the island province of Cebu was chosen as the study area due to the availability of (1) PlanetScope image (2) other reference datasets such as very high-resolution satellite image, and (3) damage taggings provided by the United Nations Satellite Center (UNOSAT) and United Nations Institute for Training and Research (UNITAR).



**Figure 1.** Pre-typhoon and post-typhoon PlanetScope images, acquired on 30 November 2021 (top) and 22 December 2021 (bottom), respectively, covering portion of Talisay City. Note the degree of damages to the natural and built environments and how these are captured by spectral and textural changes. The crosses are damage taggings from UNITAR/UNOSAT: red (damaged), yellow (potentially damaged).

Two relatively cloud-free PlanetScope (reflectance) images of Talisay City acquired on 30 November 2021 (pre-typhoon) and 22 December 2021 (post-typhoon) were used. These were obtained from Planet as part of their support to research and

development. Figure 1 shows these two images of the part of Talisay City. The following can be noted: illumination is different between the two images, damages in vegetation are clearly seen through spectral (color) changes, and damages in structures (buildings, houses) can be inferred from changes in the spatial pattern of colors.

## 2. METHODOLOGY

Damages to built and natural environments are essentially changes that needs to be detected and quantified. This is particularly true for the change detection approach. While the use of vegetation indices is effective for such assessment in natural or vegetated areas, the use of built-up indices does not yield useful results. This is because there is usually no significant change or reduction in materials. However, typhoon-damaged buildings are usually characterized by a change in form, shape, color, and texture.

Figure 2 illustrates the methodology used in this study. At least two PlanetScope images are selected, one pre-typhoon and another which is post-typhoon. The post-typhoon image is typically more challenging in terms of availability, quality, and varying amounts of cloud cover, among others. Post-typhoon images can be processed as they become available to be able to complete the assessment of damages in the entire municipalities and cities of interest.

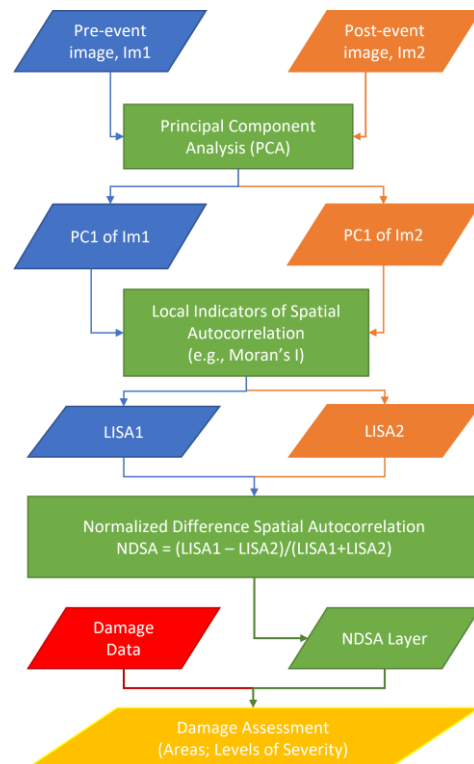


**Figure 2.** Methodological flow diagram to assess damage to buildings using bi-temporal PlanetScope images and normalized difference spatial autocorrelation (NDSA).

Each image is subjected to Principal Component Analysis (PCA). Local Indications of Spatial Autocorrelation (LISA) such as Moran's I, Geary's C, and Getis Ord are then calculated with the first Principal Components (PCs) as separate inputs. The normalized difference spatial autocorrelation is computed and examined together with available damage data (e.g.,

damage taggings from very high-resolution satellite images, post-typhoon field assessments if available)

## 2.1 Principal Component Analysis

Principal component analysis (PCA) was applied separately to the pre-typhoon and post-typhoon images. PCA is data dimensionality reduction technique, transforming the originally larger dataset into a smaller dataset whose components are uncorrelated (Jolliffe, Cadima, 2016). These resulted to four PC bands, representing uncorrelated information about the area. The first Principal Component (PC1) image essentially represent a greyscale version of the combination of most information contained in the original four bands of the PlanetScope images. Subsequent operations were conducted using PC1 images only.

## 2.2 Normalized Difference Spatial Autocorrelation

In this study, the use of spatial autocorrelation (SA) to capture and quantify these changes between two PlanetScope images (pre-typhoon and post-typhoon) was examined. The concept of normalized differenced spatial autocorrelation (NDSA) is introduced. Local SA is quantified using local Moran's I for image 1 (pre-typhoon) and image 2 (post-typhoon). The Moran's I index examined the differences in data values between neighboring pixels to the standard deviation. This provides a measure of local homogeneity. The Moran's I ranges from -1 and +1, where -1 indicates strong negative autocorrelation (i.e., there is high variance in pixel values within the neighborhood considered, patterns appears like a checkerboard), 0 means the values are spatially uncorrelated (i.e., pixel values are random), and +1 points to a strong spatial positive autocorrelation (i.e. nearby observations have similar values; clusters of similar values) (Legendre, Legendre, 1998, Jolliffe, Cadima, 2016). This Local Indicator of Spatial Autocorrelation (LISA) statistic (see Anselin, 1995) was found to be sensitive to slight differences in pixel values and can identify statistically significant spatial outliers (Liu et al., 2021). NDSA is the calculated as the difference between the two local Moran's I (pre-typhoon - post-typhoon) divided by their sum. The use of other LISA statistics, namely, local Geary's C (see Anselin, 1995, Anselin, 2019) and local Getis Ord (see Getis, Ord, 1992, Ord, Getis, 1995), was also examined. All were calculated using the Queen's rule, which takes into consideration all the 8 neighboring pixels. In this study, the evaluation of the effect of increasing lags was not considered yet as the interest is on detecting damage in as much detail possible.

# 3. RESULTS AND DISCUSSION

## 3.1 Principal Component Images

Figure 3 shows the principal component images generated by PCA. Note that damages can be identified visually as change in color, particularly for severely or completely damaged structures. In the first PC images, the damaged buildings can be identified by looking at, generally, the reduction in brightness values. However, the damages and their variation in terms of "severity" can be better identified by utilizing textural information.

It should be noted that the damage taggings are not exhaustive. Due to several reasons (e.g., cloud cover, poor image quality), several damaged buildings may have not been tagged. We can

see this in Figure 3, where there are discernible changes but were not tagged as damaged or potentially damaged.

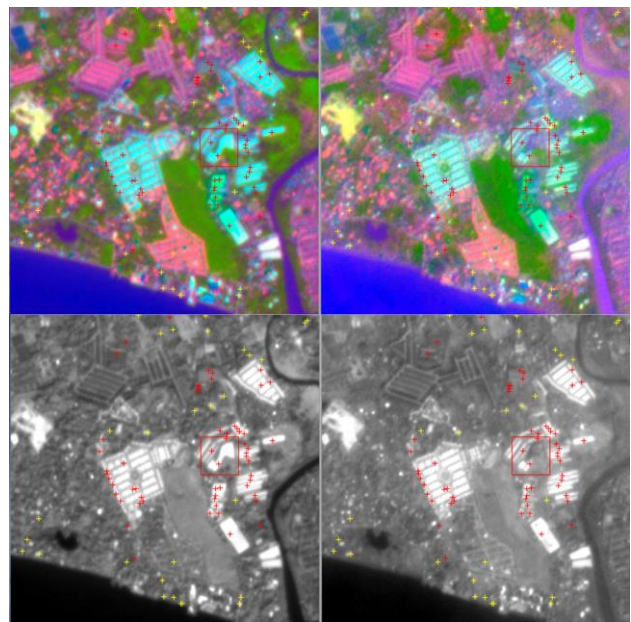


**Figure 3.** False color composite based on RGB PC3-PC1-PC2 (top) and PC1 images (bottom) corresponding to the pre-typhoon (left) and post-typhoon (right) images. Damage buildings and other areas can be seen as change in color and texture.

## 3.2 LISA and NDSA layers

The layers for local Moran's I, Getis-Ord Gi, and Geary's C for pre- and post-typhoon are shown in Figure 4. Local Moran's I values for damaged buildings are lower compared to those of buildings which are not impacted significantly. This indicates reduced homogeneity of values within the spatial neighborhood considered (spatial lag = 1). Intact roofs are expected to be homogeneous as values are similar due to same materials, same color, same orientation, and other possible cause of relatively high homogeneity. As the roof and other parts of a building becomes damaged, surfaces may get more deformed and other material may be exposed. These results to a more heterogenous set of pixel values and therefore, lower local Moran's I.

Based on the local Getis-Ord Gi images shown in Figure 4, similar observations can be made. Reduction in local Getis-Ord Gi values can be used to identify affected areas. However, in contrast with the local Moran's I, this LISA statistic can also identify clusters of high-low values and clusters of low-high values. This, as it relates to degree and nature of damage, will have to be explored further in another study.

The local Geary's C layers appear different compared to local Moran's I and local Getis-Ord Gi (Figure 4). Boundaries and edges have high values of Geary's C. These are areas of high dissimilarity or negative spatial autocorrelation.

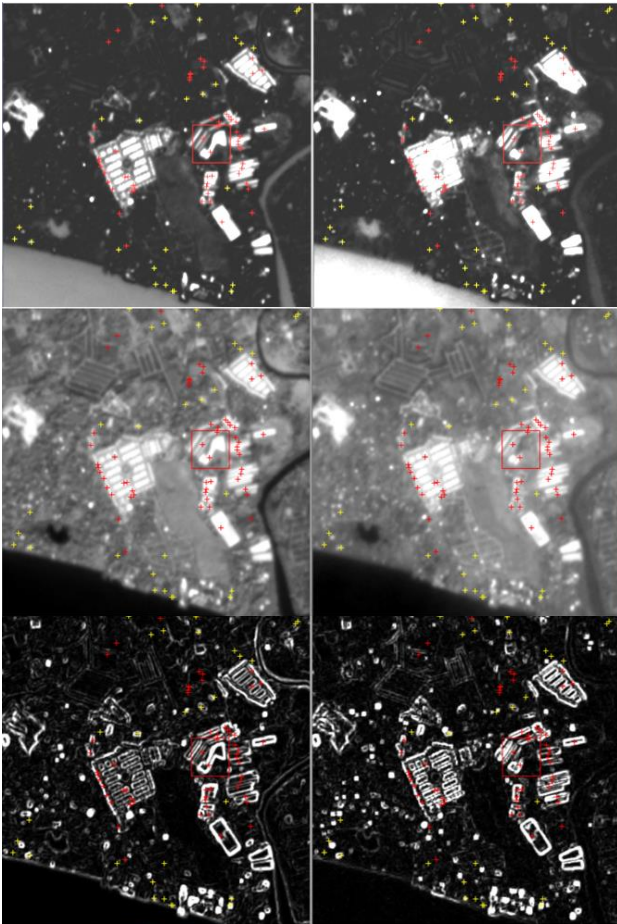


**Figure 4.** LISA layers for pre-typhoon and post-typhoon using Moran's I (top), Getis-Ord Gi (middle), and Geary's C (bottom).

Figures 5 to 7 show the NDSA layers based of the three LISA statistics. The higher levels of damage are show in red and orange. Overall, the general spatial distributions of the various levels of damage appear similar. The NDSA local Moran's I (Figure 5) and NDSA local Getis-Ord Gi (Figure 6) are highly similar with the latter appearing to be a regionalized version of the former. On the other hand, more granularity can be seen in NDSA local Geary's C (Figure 7). Note that there are identified areas (blue and green) in NDSA local Moran's I and NDSA local Getis-Ord Gi that are not capture in the NDSA local Geary's C.

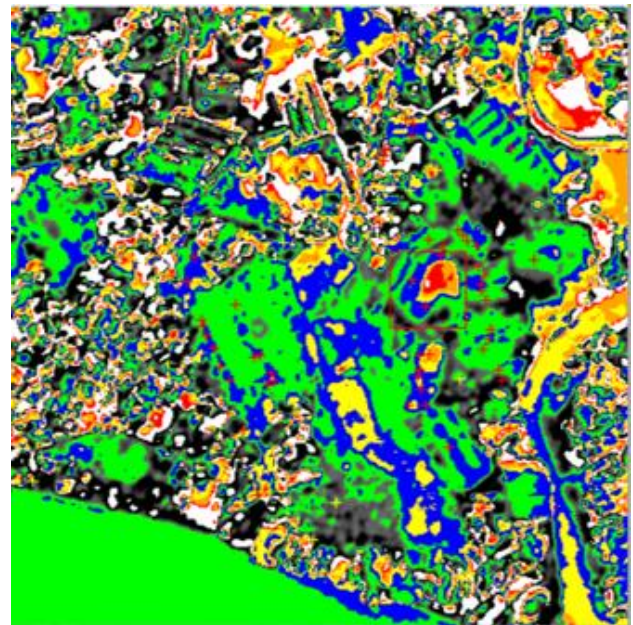


**Figure 6.** NDSA layer using Getis-Ord Gi:  $>0-0.2$  (green),  $0.2-0.4$  (blue),  $0.4-0.6$  (yellow),  $0.6-0.8$  (orange),  $0.8-1.0$  (red). Green to red indicates increasing levels of damage.

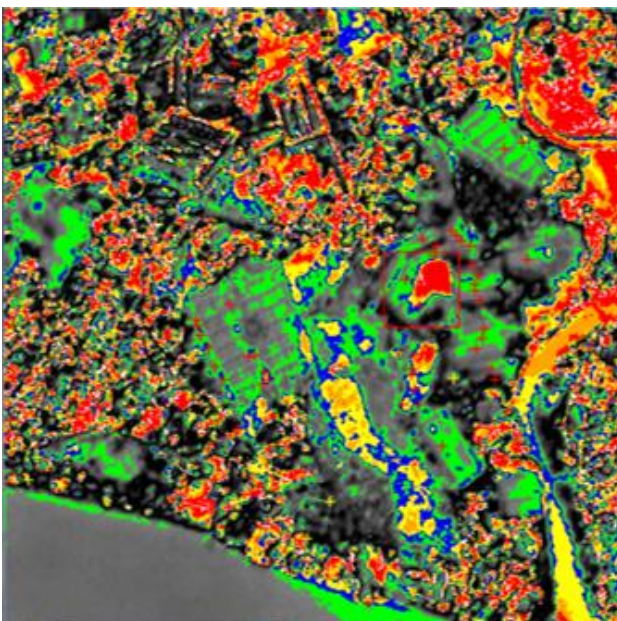


**Figure 5.** NDSA layer using local Moran's I:  $>0-0.2$  (green),  $0.2-0.4$  (blue),  $0.4-0.6$  (yellow),  $0.6-0.8$  (orange),  $0.8-1.0$  (red). Green to red indicates increasing levels of damage.

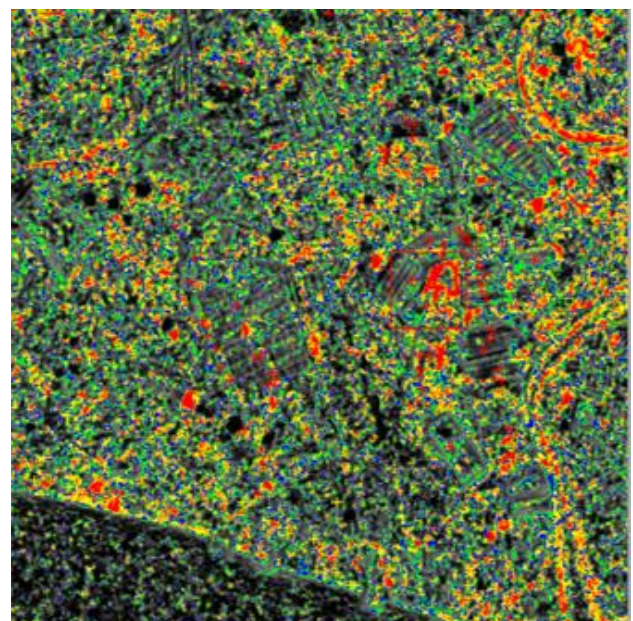


**Figure 7.** NDSA layer using local Geary's C:  $>0-0.2$  (green),  $0.2-0.4$  (blue),  $0.4-0.6$  (yellow),  $0.6-0.8$  (orange),  $0.8-1.0$  (red). Green to red indicates increasing levels of damage.

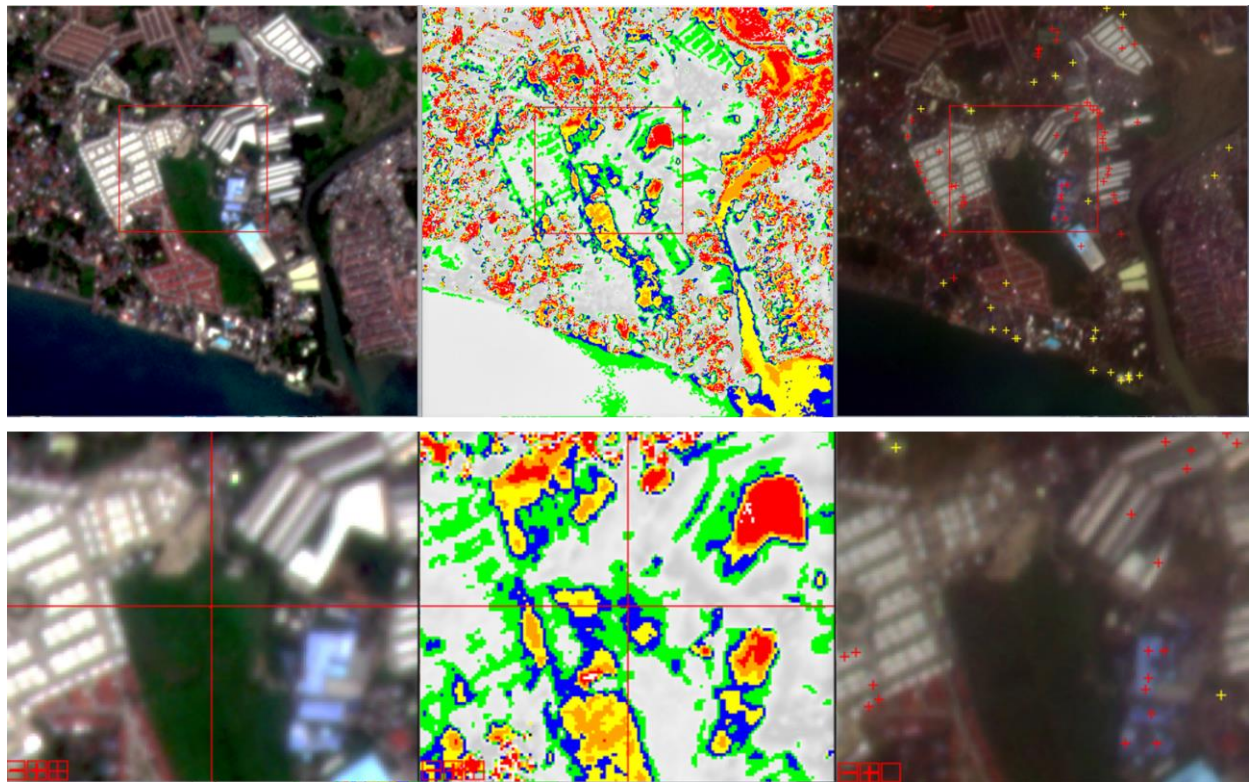


**Figure 8.** Damage assessment layer (middle) based on NDSA local Moran's I (red: 0.8-1.0, orange: 0.6-0.8, yellow: 0.4-0.6, blue: 0.2-0.4, green: >0-0.2) derived from pre-typhoon and post-typhoon PlanetScope images covering portion of Talisay City. Images at the second row are zoom-ins of area within red box on images in the first row.

### 3.3 Correspondence between NDSA and Level of Damage

With the observation that SA generally decreases due to damages (especially to manmade structures), positive NDSA identifies the damage areas. Figure 2 shows the NDSA-based damage assessment map generated from the pre- and post-typhoon PlanetScope images. The points representing manually tagged damaged and potentially damaged buildings are also shown. These were provided by UNITAR/UNOSAT. In general, the points coincided with positive values of NDSA. Moreover, the magnitude of the values corresponded to the level or degree of damage sustained as interpreted from very high-resolution satellite image.

In Figure 3, we can see that yellow to red areas in the NDSA maps indicate severe damage to destruction of the structures. The blue and green areas represent those which are relatively less damaged. It is interesting to note that the manual tagging of damages had missed buildings which are clearly damaged or destroyed based on the visual comparison of pre- and post-typhoon satellite images. This illustrates the value of the NDSA not only to assess damage on its own but also for guiding manual tagging from image and prioritizing post-disaster needs assessment and recovery operation.

In this study, the NDSA was applied to the entire image, that is, NDSA was computed also for the vegetation areas and other natural features. For the natural environment, the absolute value of NDSA indicate corresponding degrees of damage based on visual interpretation of very high-resolution satellite image. Damages to specific feature type or land cover class can be easily carried out using thresholding of indices such as the

normalized difference vegetation index (NDVI) and the normalized difference built-up index (NDBI).

### 3.4 Limitations

The approach requires that pre- and post-damage images. This may pose as problem in some cases where pre-damage images are not available. Saito and Spence (2004) recognized this by developing a damage assessment method that only utilizes post-damage image.

## 4. CONCLUSIONS AND FUTURE WORK

### 4.1 Conclusions

Through NDSA, damaged (high NDSA values) and potentially damaged areas (relatively low NDSA values) were mapped. It is apparent that the magnitude of NDSA values can be used as measure of the degree of damage. Each of the LISA statistics, namely, Local Moran's I, local Getis-Ord  $G_i^*$ , and local Geary's  $C$ , can be used as basis for the NDSA. However, considering their complementarity with each other, they can all be used for guiding the identification of damaged areas considering "severity" levels.

### 4.2 Future Work

Further work is being done to examine values of NDSA in damages built-up and natural/vegetated areas. More damage taggings are needed to quantitatively assess NDSA ranges vis-à-vis damage levels/severity. Other local measures of autocorrelation can be further evaluated. As mentioned, local

SA at various spatial lags should also be examined. However, the sizes of the features of interest (e.g., buildings and houses) must be considered so as not to make the interpretation of NDSA difficult with the combination of built and non-built features in the calculation of SA. Textural measures (e.g., grey level co-occurrence matrix) can also be explored. The work of Lui and Li (2019) seems promising for application to PlanetScope images as well.

As spatial autocorrelation and other measures evaluation structure and texture can be affected by image quality, conditions during image acquisitions, it would be interesting to assess the impact of these so that the robustness of these indices can be tested. More importantly, it would be good to reduce the effects of poor image quality resulting from various factors including environmental conditions.

### ACKNOWLEDGEMENTS

The author is grateful for the PlanetScope images and damage tagging data provided by Planet and UNITAR/UNOSAT, respectively.

### REFERENCES

- Anselin, L. (1995) Local Indicators of Spatial Association — LISA. *Geographical Analysis* 27: 93–115.
- Anselin, L. (2019) A Local Indicator of Multivariate Spatial Association, Extending Geary's c. *Geographical Analysis* 51 (2): 133–50.
- Antonietta, F., Boccardo, P., Tonolo, F.G., Vassileva, M. (2015) Damage assessment exploiting remote sensing imagery: Review of the Typhoon Haiyan Case Study. 2015 IEEE International Geoscience and Remote Sensing Symposium (IGARSS), 3556-3559
- Adriano (2019) Multi-source data fusion based on ensemble learning for rapid building damage mapping during the 2018 Sulawesi earthquake and tsunami in Palu, Indonesia. *Remote Sensing* 11, 886
- Boschetti, M. (2015) Rapid assessment of crop status: An application of MODIS and SAR data to rice areas in Leyte, Philippines affected by Typhoon Haiyan. *Remote Sensing* 7(6), 6535-6557
- Getis, A., Ord, J.K. (1992) The Analysis of Spatial Association by Use of Distance Statistics. *Geographical Analysis* 24: 189–206.
- Griffith, D.A. (1987) Spatial autocorrelation. In *A Primer; Association of American Geographers*: Washington, DC, USA
- Hoque, M.A. (2017) A systematic review of tropical cyclone disaster management research using remote sensing and spatial analysis. *Ocean & Coastal Management* 146, 109-120
- Jimenez-Jimenez, S.I., Ojeda-Bustamante, W., Ontiveros-Capurata, R.E., Marcial-Pablo, M.d.J. (2020) Rapid urban flood damage assessment using high resolution remote sensing data and an object-based approach. *Geomatics, Natural Hazards and Risk* 11:1, 906-927
- Jolliffe, I. T., Cadima, J. (2016). Principal Component Analysis: a Review and Recent Developments. *Phil. Trans. R. Soc. A.* 374, 20150202. doi:10.1098/rsta.2015.0202
- Liu, J., Li, P. (2019) Extraction of Earthquake-Induced Collapsed Buildings from Bi-Temporal VHR Images Using Object-Level Homogeneity Index and Histogram. *IEEE Journal of Selected Topics in Applied Earth Observations and Remote Sensing*, vol. 12, no. 8, pp. 2755-2770, doi: 10.1109/JSTARS.2019.2904670.
- Legendre, P., Legendre, L. (1998). *Numerical ecology. Developments in environmental modelling*, vol. 20 (pp. 1– 853). Amsterdam' Elsevier.
- Liu, C., Sui, H., Huang, L. (2021) Identification of Damaged Building Regions from High- Resolution Images Using Superpixel-Based Gradient and Autocorrelation Analysis. *IEEE Journal of Selected Topics in Applied Earth Observations and Remote Sensing* 14, 1010-1024
- McCarthy (2020) Mapping hurricane damage: A comparative analysis of satellite monitoring methods. *International Journal of Applied Earth Observation and Geoinformation* 91
- Mondini, A.C. (2017) Measures of Spatial Autocorrelation Changes in Multitemporal SAR Images for Event Landslides Detection. *Remote Sensing* 2017, 9, 554; doi:10.3390/rs9060554
- Ord, J.K., Getis, A. (1995) Local Spatial Autocorrelation Statistics: Distributional Issues and an Application. *Geographical Analysis* 27: 286–306.
- Plank, S., 2014. Rapid Damage Assessment by Means of Multi-Temporal SAR — A Comprehensive Review and Outlook to Sentinel-1. *Remote Sensing* 6(6), 4870-4906. doi.org/10.3390/rs6064870.
- Saito, K., Spence, R. (2004), Rapid damage mapping using post-earthquake satellite images, IGARSS 2004. 2004 IEEE International Geoscience and Remote Sensing Symposium, 2004, pp. 2272-2275 vol.4, doi: 10.1109/IGARSS.2004.1369737
- Tay, C.W.J. (2020) Rapid flood and damage mapping using synthetic aperture radar in response to Typhoon Hagibis, Japan. *Scientific Data* 7:100
- Vijayaraj, V., Bright, E.A., Bhaduri, B.L. (2008) Rapid Damage Assessment from High Resolution Imagery, IGARSS 2008 - 2008 IEEE International Geoscience and Remote Sensing Symposium, 2008, pp. III - 499-III - 502, doi: 10.1109/IGARSS.2008.4779393.
- Xu, J. Z., Lu, W., Li, Z., Khaitan, P., Zaytseva, V. (2019) Building Damage Detection in Satellite Imagery Using Convolutional Neural Networks. 33rd Conference on Neural Information Processing Systems (NeurIPS 2019). arXiv:1910.06444v1
- Yamazaki, F. and Matsuoka, M. (2007) Remote sensing technologies in post-disaster damage assessment. *Journal of Earthquake and Tsunami* 1:3, 193-210
- Zhou, Z.G.; Tang, P.; Zhou, M. (2016) Detecting anomaly regions in satellite image time series based on seasonal autocorrelation analysis. *ISPRS Ann. Photogramm. Remote Sens. Spat. Inf. Sci.* 2016, III-3, 303–310.